Inorganic Chemistry
Article
Cite This: *Inorg. Chem.* XXXX, XXX, XXX−XXX
pubs.acs.org/IC

TiO_2@UiO-68-CIL: A Metal−Organic-Framework-Based Bifunctional Composite Catalyst for a One-Pot Sequential Asymmetric Morita−Baylis−Hillman Reaction

Yu-Hong Hu,[†] Cong-Xue Liu,[†] Jian-Cheng Wang,* Xiu-Hui Ren, Xuan Kan, and Yu-Bin Dong*

College of Chemistry, Chemical Engineering and Materials Science, Collaborative Innovation Centre of Functionalized Probes for Chemical Imaging in Universities of Shandong, Key Laboratory of Molecular and Nano Probes, Ministry of Education, Shandong Normal University, Jinan 250014, P. R. China

Supporting Information

ABSTRACT: A chiral ionic liquid (CIL) moiety of a L-pyrrolidin-2-ylimidazole-decorated homochiral UiO-68-type metal−organic framework, UiO-68-CIL (**1**), was successfully prepared by the combination of a new premodified chiral CIL ligand (**H_2L-CIL**) and $ZrCl_4$ via a solvothermal method. The TiO_2-loaded TiO_2@UiO-68-CIL (**2**) was prepared by impregnating **1** in a toluene solution of $Ti(OPr^i)_4$ and sequential in situ hydrolysis. The obtained **2** can be a bifunctional asymmetric heterogeneous catalyst to successfully promote the one-pot Morita−Baylis−Hillman reaction starting from aromatic alcohols in a tandem way.

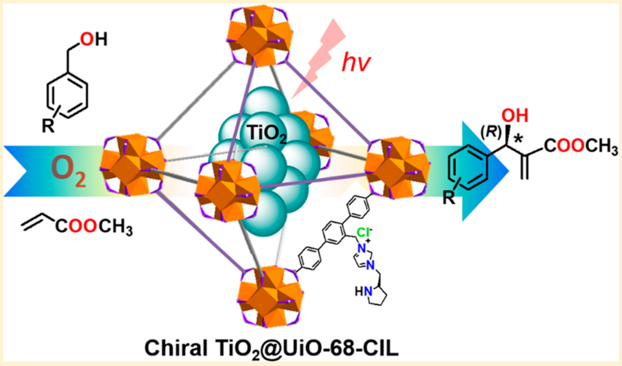

INTRODUCTION

Metal−organic frameworks (MOFs), as a promising class of porous supports, have been widely used in the fabrication of composite catalytic systems for heterogeneous organic transformations.[1−3] To date, various inorganic catalytic active species such as metal nanoparticles (M NPs) or metal oxides,[4−16] inorganic metal salts,[17−21] and even nonmetal components[22,23] have successfully been loaded by MOF platforms. On the other hand, active organocatalytic functional moieties, like the functionalized ionic liquid (IL),[24−27] can also be covalently grafted onto MOFs via a direct ligand modification or a postsynthetic approach to generate MOF-based heterogeneous organocatalytic systems.[19,28−31] In view of the synthetic methodology, both inorganic and organic catalytic species, together with chirality, could be simultaneously incorporated into MOF platforms; consequently, the distinctly different types of catalytic species would be integrated together to enable new functionality.

In this contribution, we report for the first time such a chiral ionic liquid (CIL)-involved and TiO_2-loaded MOF-based composite bifunctional catalyst, namely, TiO_2@UiO-68-CIL (**2**). It was prepared by loading TiO_2 via hydrolysis of its precursor $Ti(OPr^i)_4$, which was preembedded in a chiral UiO-68-CIL (**1**) MOF matrix by solution impregnation. The obtained **2** can be a highly efficient and heterogeneous catalyst to promote the one-pot sequential asymmetric Morita−Baylis−Hillman (MBH) reaction starting from alcohol under ambient conditions.

We incorporated chiral **1** with TiO_2 into a TiO_2@MOF system based on the following reasons: first, TiO_2 is known to be one of the most important photoactive species in photocatalysis,[32−42] especially in photocatalytic oxidation; second, ILs, as an important class of organocatalysts, have been proven to be highly efficient in catalyzing a number of chemical transformations such as acid- or base-mediated organic reactions;[24−27] third, chirality could be readily achieved during ligand synthesis[43−46] via CIL decoration. Hopefully, the incorporation of photoactive TiO_2 and CIL organocatalytic species along with the chiral function into MOF platforms would generate a composite multifunctional asymmetric catalytic system for organic transformations in a tandem way.

EXPERIMENTAL SECTION

Materials and Instrumentations. All of the chemicals were obtained from commercial sources (Acros) and used without further purification. The detailed synthetic procedure for the chiral ligand of **H_2L-CIL** is shown in Supporting Information. ^1H NMR data were collected on a Bruker Avance-400 spectrometer. Chemical shifts are reported in δ relative to tetramethylsilane. IR spectra were obtained in the 400−4000 cm^{-1} range using a Bruker Alpha Fourier transform infrared (FT-IR) spectrometer. Elemental analyses were performed on a PerkinElmer model 2400 analyzer. Inductively coupled plasma (ICP) measurement was conducted on an IRIS Intrepid (II) XSP and NU AttoM spectrometer. High-resolution mass spectrometry (MS)

Received: July 28, 2018

DOI: 10.1021/acs.inorgchem.8b02132

Scheme 1. Synthesis of H_2L-CIL, 1, and 2

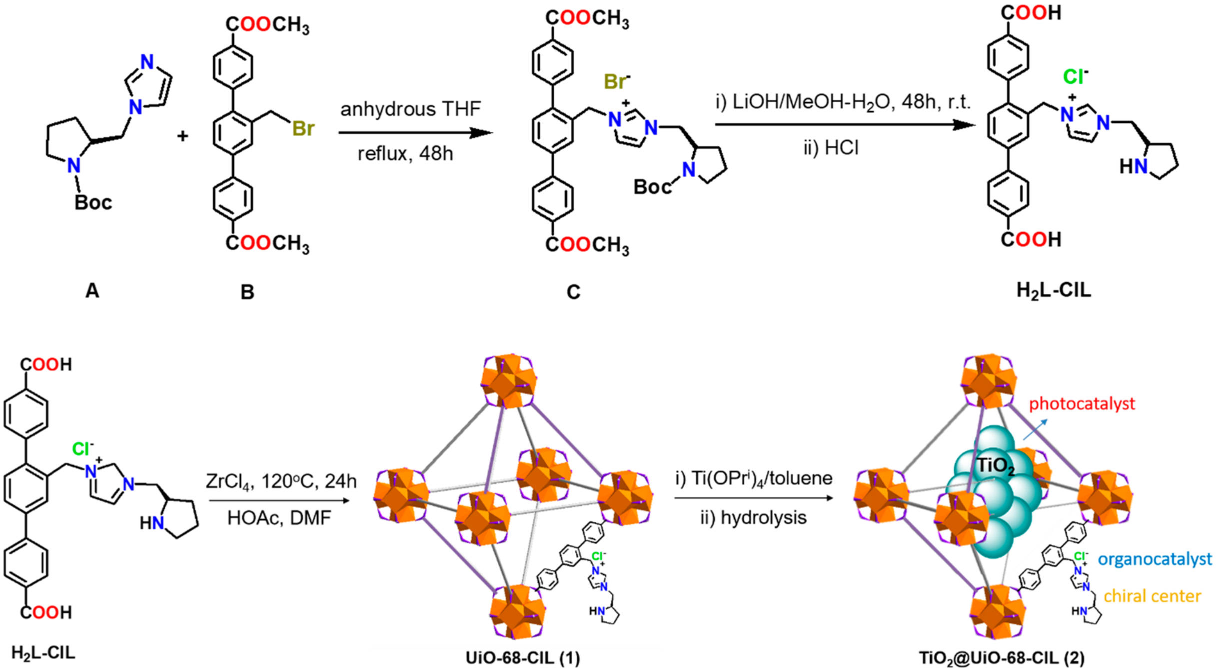

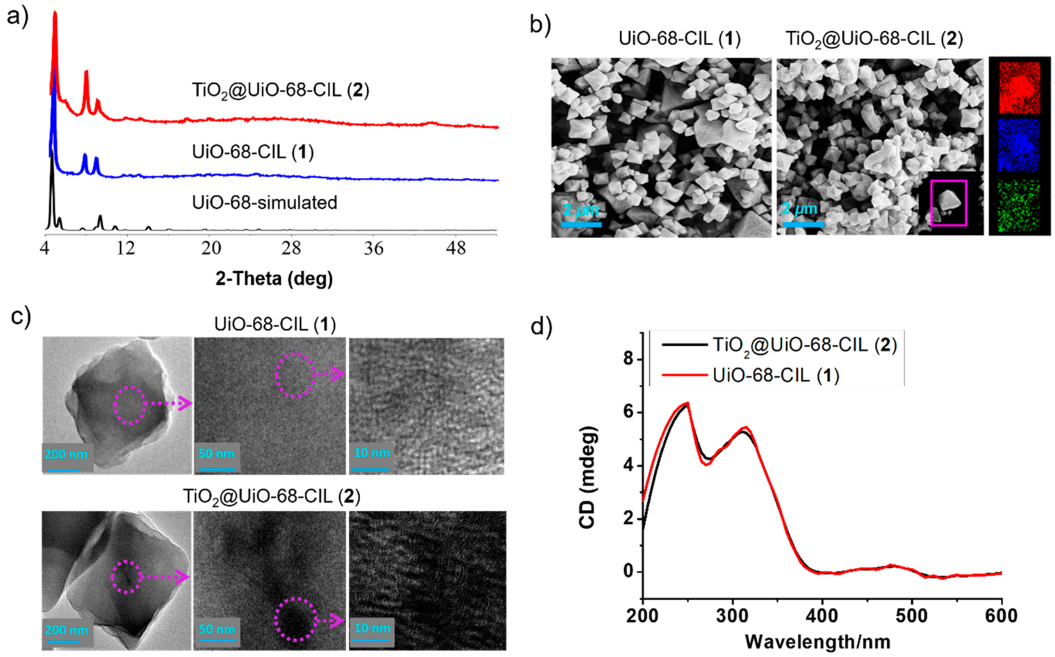

Figure 1. (a) PXRD patterns of the simulated UiO-68, **1**, and **2**. (b) SEM images of **1** and **2** and EDS elemental mapping of **2**. (c) TEM images of **1** and **2**. (d) CD spectra of **1** (red line) and **2** (black line).

analysis was carried out on a Bruker Maxis ultrahigh-resolution quadrupole time-of-flight mass spectrometer. Thermogravimetric analysis (TGA) was performed on a TA Instrument Q5 analyzer under flowing nitrogen at a heating rate of 10 °C/min. Powder X-ray diffraction (PXRD) patterns were obtained on a D8 ADVANCE powder X-ray diffractometer with Cu Kα radiation (λ = 1.5405 Å). A 300 W xenon lamp (PLS-SXE300C, Perfect light Co., Beijing, China) was used as the light source. Scanning electron microscopy (SEM) micrographs were recorded on a Gemini Zeiss Supra TM scanning electron microscope equipped with an energy-dispersive X-ray detector.

*Synthesis of **1**.* $ZrCl_4$ (57.6 mg, 0.24 mmol) and 50 equiv of acetic acid (0.68 mL) were dissolved in *N*,*N*-dimethylformamide (DMF; 10 mL) by using ultrasound (30 min). **H_2L-CIL** (124.4 mg, 0.24 mmol) was added to the obtained clear solution in an equimolar ratio related to $ZrCl_4$. The tightly capped flasks were kept in an oven at 90 °C under static conditions. After 24 h, the reaction system was allowed to cool to room temperature and the generated precipitate was collected by centrifugation. The solids were suspended in fresh DMF (20 mL). After the solution was allowed to stand at room temperature for 10 h, the suspension was centrifuged and the solvent was decanted off. The obtained MOF micronanoparticles were completely washed with ethanol (20 mL) several times. Finally, the solids were dried in a vacuum to generate **1**. Yield: 74.1%. IR (KBr pellets, cm^{-1}): 3378(w), 1592(s), 1544(ms), 1417(vs), 1183(w), 1148(w), 1006(w), 836(w), 780(ms), 712(w), 649(w). Elem anal. Calcd for C_{174} H_{160} O_{32} N_{18} Zr_6: C, 55.18; H, 4.58; N, 6.66. Found: C, 55.08; H, 4.37; N, 6.91.

*Synthesis of **2**.* In a nitrogen atmosphere, **1** (124.3 mg, 0.032 mmol) was added to a $Ti(OPr^i)_4$ (33.3 μL, 0.109 mmol) solution of anhydrous toluene (7 mL) at 100 °C. The mixture was stirred at this temperature for an additional 1 h. The obtained crystalline solids were consecutively washed with toluene, ethanol, water (H_2O), ethanol, and diethyl ether. Then, the solids were dried at 80 °C for 2 h to afford **2**. IR (KBr pellets, cm^{-1}): 3370(w), 1606(s), 1548(ms), 1417(vs), 1183(w), 1146(w), 1006(w), 836(w), 780(ms), 712(w), 649(w). Elem anal. Calcd for $C_{174}H_{160}O_{39.58}N_{18}Zr_6Ti_{3.79}$: C, 54.02; H, 4.14; N, 6.52. Found: C, 54.29; H, 4.39; N, 6.47. The formula of **2** was described as $3.79TiO_2$@UiO-68-CIL based on the elemental analysis and ICP results (Table S1).

General Procedure for Photoinduced Alcohol Oxidation Catalyzed by 2. A 300 W xenon lamp was used as the visible-light source in the experiment. In an oxygen atmosphere, a mixture of $ArCH_2OH$ (1 mmol), methanol (MeOH; 5 mL), and **2** (0.02 mmol) was stirred at room temperature for 24 h [monitored by thin-layer chromatography (TLC)] to afford the corresponding aldehydes. The yield was determined by gas chromatography (GC) measurement on an DB-5 column.

General Procedure for a MBH Reaction Catalyzed by 2. A mixture of ArCHO (1 mmol), methyl acrylate (1.2 mmol), MeOH (5 mL), and **2** (0.02 mmol) was stirred at room temperature for 48 h (monitored by TLC) to afford the corresponding products. Yields were determined by GC measurement on a DB-5 column.

General Procedure for a One-Pot MBH Reaction Catalyzed by 2. A 300 W xenon lamp was used as the visible-light source in the experiment. In an oxygen atmosphere, a mixture of $ArCH_2OH$ (1 mmol), MeOH (5 mL), and **2** (0.02 mmol) was stirred at room temperature for 24 h. After the addition of methyl acrylate (1.2 mmol), the light source was removed, and the mixture was stirred at room temperature for an additional 48 h. After the reaction, **2** was recovered by centrifugation, and the solvent was removed in a vacuum. The crude products were purified by a column on silica gel to afford the corresponding products (Supporting Information).

RESULTS AND DISCUSSION

Synthesis and Characterization of H_2L-CIL. As shown in Scheme 1, a chiral ligand precursor of **C** was prepared in 80% yield by quaternization of the L-pyrrolidineimidazole (**A**) with α-bromomethyl and dicarboxylic acid dimethyl ester substituted *p*-terophenyl (**B**) in anhydrous tetrahydrofuran (THF) under reflux for 48 h. Dicarboxylic ligand **H_2L-CIL** was obtained via hydrolyzation of **C** with LiOH in a MeOH/H_2O mixed solvent system at room temperature in 86% yield. The corresponding ^{1}H NMR, FT-IR, and MS spectra for **A**−**C** and **H_2L-CIL** are provided in the Supporting Information.

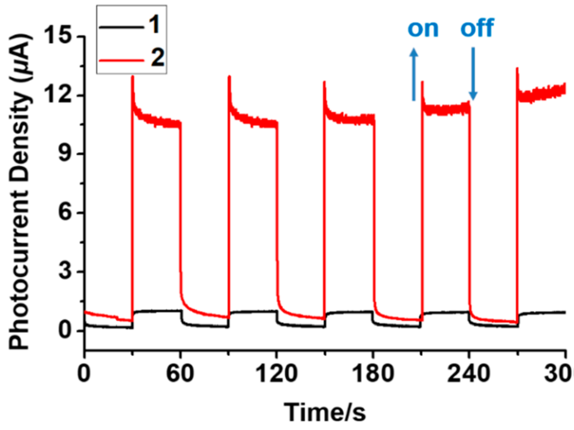

Figure 2. Transient photocurrents of **1** (black line) and **2** (red line).

Table 1. Model Photocatalytic Benzyl Alcohol Oxidation[a]

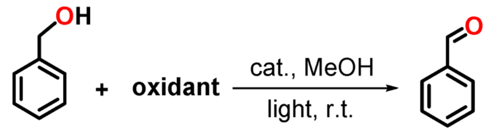

entry	light source	catalyst	solvent	oxidant	time (h)	yield (%)[b]
1		**2**	MeOH	oxygen	24	<1
2	sun light	**2**	MeOH	oxygen	24	11
3	xenon lamp	**2**	MeOH	oxygen	24	78
4	xenon lamp	**2**	MeOH	air	24	21
5	xenon lamp	**2**	CH_3CN	oxygen	24	77
6	xenon lamp	**2**	H_2O	oxygen	24	46
7	xenon lamp	**2**	THF	oxygen	24	68
8	xenon lamp	**1**	MeOH	oxygen	24	<1
9	xenon lamp	amorphous TiO_2	MeOH	oxygen	24	10
10	xenon lamp	**1**/amorphous TiO_2	MeOH	oxygen	24	<12

[a] Reaction conditions: alcohol (0.2 M) in MeOH (5 mL), catalyst (1 mmol %), oxygen or air atmosphere (1 atm), room temperature, light irradiation (300 W xenon lamp; λ > 400 nm; intensity = 75−95 × 103 lx). [b] Yields were determined by GC.

Table 2. Photocatalytic Oxidation of Different Benzyl Alcohols Catalyzed by 2[a]

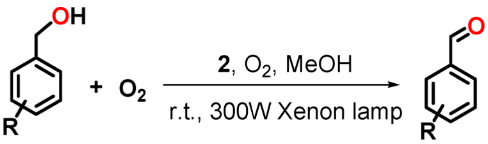

entry	R	time (h)	yield (%)[b]
1	H−	24	78
2	2-MeO−	24	93
3	3-MeO−	24	90
4	4-MeO−	24	>99
5	2-Me−	24	88
6	3-Me−	24	86
7	4-Me−	24	93
8	2-NO_2−	24	41
9	3-NO_2−	24	35
10	4-NO_2−	24	45

[a] Reaction conditions: alcohol (1.0 mmol), CH_3OH (5 mL), catalyst (2 mol % **2**, 7.5 mol % TiO_2 equiv), oxygen atmosphere (1 atm), room temperature, and 300 W xenon lamp (λ > 400 nm; intensity = 75−95 × 103 lx). [b] Yields were determined by GC.

Synthesis and Characterization of UiO-68-CIL (1) and TiO_2@UiO-68-CIL (2). The chiral **1** was synthesized by a combination of $ZrCl_4$ and **H_2L-CIL** under solvothermal conditions (DMF, 90 °C, 24 h) in the presence of acetic acid in 74% yield (Scheme 1). Notably, the CIL moiety was stable during the synthesis process of **1** under the given synthetic conditions (Supporting Information). TiO_2-loaded **2** was prepared by immersing **1** in a dry toluene solution of

Table 3. Model MBH Reaction Catalyzed by 2[a]

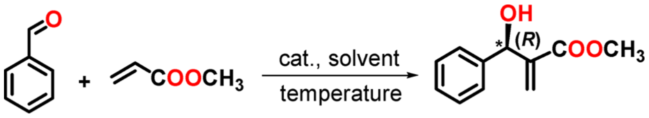

entry	T (°C)	catalyst	solvent	time (h)	yield (%)[b]	ee (%)[b]
1	25	**2**	MeOH	24	44	86
2	50	**2**	MeOH	24	79	11
3	60	**2**	MeOH	24	87	<3
4	25	**2**	MeOH	48	96	83
5	25	**2**	H_2O	48	10	83
6	25	**2**	THF	48	47	65
7	25	**2**	CH_3CN	48	66	80
8	25	**2**[c]	MeOH	48	93	64
9	25	**2**[d]	MeOH	48	96	84
10	25	**1**	MeOH	48	96	83
11	25		MeOH	48	<5	<1

[a]Reaction conditions: benzaldehyde (1.0 mmol), CH_3OH (5 mL), catalyst (2 mol %), methyl acrylate (1.0 mmol). [b]Yields and ee values were determined by GC and chiral high-performance liquid chromatography (HPLC), respectively. [c]**2** (1.5 mol %). [d]**2** (2.5 mol %).

Table 4. MBH Reaction of Acrylic Esters and Various Benzyl Aldehydes Catalyzed by 2[a]

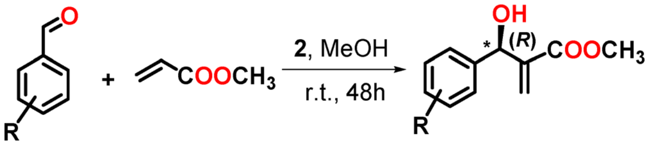

entry	R	yield (%)[b]	ee (%)[b]
1	2-MeO–	88	90
2	3-MeO–	93	97
3	4-MeO–	99	99
4	2-Me–	68	85
5	3-Me–	85	93
6	4-Me–	97	96
7	2-NO_2–	44	87
8	3-NO_2–	56	95
9	4-NO_2–	64	98

[a]Reaction conditions: benzyl aldehydes (1.0 mmol), CH_3OH (5 mL), catalyst (2 mol %), methyl acrylate (1.0 mmol), room temperature. [b]Yields and ee values were determined by GC and chiral HPLC, respectively.

Table 5. One-Pot Sequential MBH Reaction Catalyzed by 2[a]

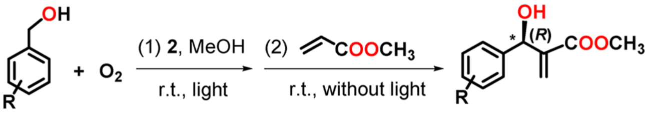

entry	R	solvent	yield (%)[b]	ee (%)[c]
1	H-	MeOH	75	83
2	2-MeO-	MeOH	67	86
3	3-MeO-	MeOH	86	95
4	4-MeO-	MeOH	99	99
5	2-Me-	MeOH	50	81
6	3-Me-	MeOH	62	90
7	4-Me-	MeOH	78	95
8	2-NO_2-	MeOH	12	85
9	3-NO_2-	MeOH	16	92
10	4-NO_2-	MeOH	27	98
11	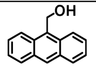 OH	MeOH	-	-

[a]Reaction conditions: (1) alcohols (1.0 mmol), CH_3OH (5 mL), catalyst (2.0 mol %), oxygen atmosphere (1 atm), and 300 W xenon lamp (λ > 400 nm; intensity = 75−95 × 103 lx), room temperature, 24 h; (2) methyl acrylate (1.0 mmol), without light, room temperature, 48 h. [b]Isolated yield. [c]The ee values were determined by chiral HPLC (Supporting Information).

$Ti(OPr^i)_4$ (100 °C, 1 h), followed by an in situ hydrolysis step for the uploaded $Ti(OPr^i)_4$ during the H_2O-washing process (Scheme 1).[47]

The PXRD patterns indicated that **1** and **2** are highly crystalline and their structures are identical with that of pristine UiO-68 (Figure 1a).[48,49] So, the loaded TiO_2 and L-pyrrolidin-2-ylimidazole-decorated **H_2L-CIL** did not destroy and influence formation of the UiO-68 framework under the reaction conditions. On the other hand, we did not observe the characteristic peaks for crystalline TiO_2 in the PXRD pattern of **2**, indicating that the encapsulated TiO_2 in the MOF existed in its amorphous form.[50] SEM measurement showed that both **1** and **2** were obtained as micronanoparticles with octahedral shape (Figure 1b). The energy-dispersive X-ray spectroscopy (EDS) measurement (Figure 1b) showed that the loaded TiO_2 evenly distributed in **2**. The uploaded TiO_2 amount in **2** was determined by ICP measurement (Supporting Information), and the Zr/Ti ratio in **2** was 1.57:1.00; therefore, the corresponding formula of **2** can be described as 3.79TiO_2@UiO-68-CIL, which was further supported by elemental analysis. The encapsulated TiO_2 species in **2** was further investigated by high-resolution transmission electron microscopy (HRTEM). As shown in Figure 1c, the amorphous titania layers are present in the MOF matrix of **2**,[51,52] which was not observed in **1**. Moreover, in **1** and **2**, the chiral feature of the L-pyrrolidine species was retained, which was well supported by the solid circular dichroism (CD) measurement. The CD spectra of **1** and **2** unambiguously confirmed the enantiomeric nature of the optical activity. As indicated in Figure 1d, **2** showed positive dichroic signals at 250 and 310 nm in its CD spectrum, which is basically identical with that of **1**. The framework of **2** was stable up to ca. 160 °C based on TGA and PXRD measurements (Supporting Information), so it was stable enough to promote organic transformations under mild reaction conditions.

Through measurement of the nitrogen gas (N_2) adsorption at 77 K, we obtained the permanent porosity of **2**. Unlike pure UiO-68, **2** exhibited typical type IV behavior (Supporting Information), which should be caused by the introduced CIL groups and loaded TiO_2. There was pore condensation with pronounced adsorption−desorption hysteresis (the pore

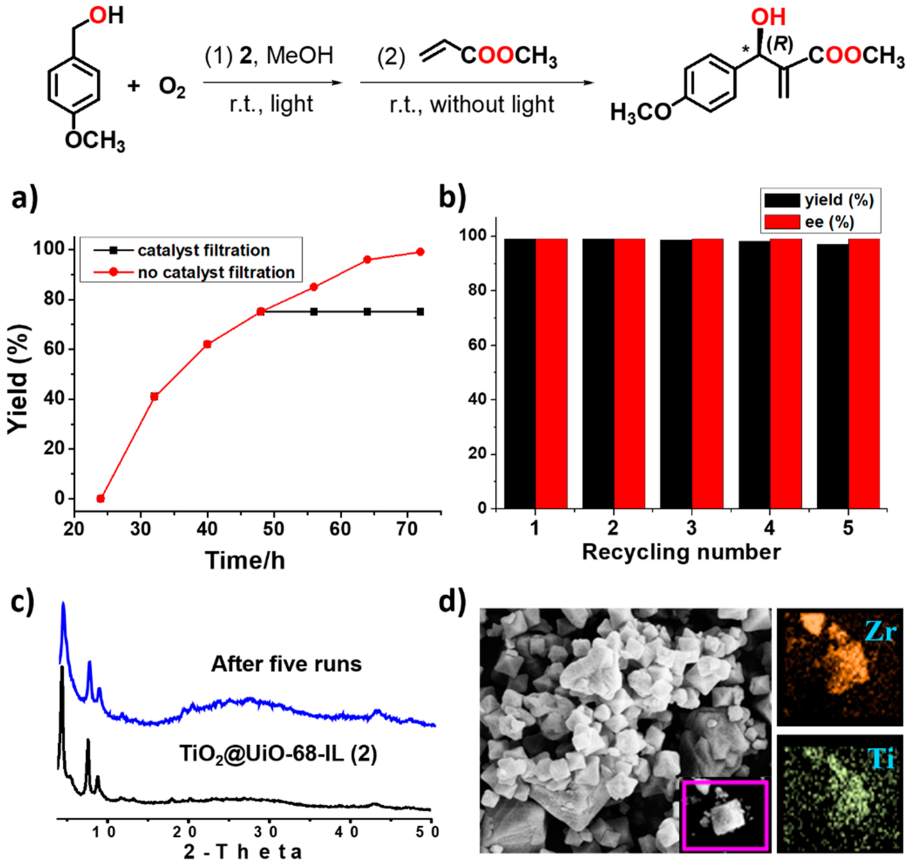

Figure 3. (a) Reaction time examination (red line) and leaching test (black line) for the one-pot tandem model reaction catalyzed by **2**. (b) Recycling test for the one-pot stepwise reaction based on 4-methoxybenzyl alcohol and methyl acrylate catalyzed by **2**. (c) PXRD patterns of as-synthesized **2** and after five catalytic runs. (d) SEM image and EDS elemental mapping of **2** after five catalytic cycles.

widths were centered at ca. 8.5 Å; Supporting Information). These results indicated the existence of mesopores in **2** with a maximum N_2 uptake of 592 cm^3/g (a Brunauer−Emmett−Teller surface area of 223 m^2/g), but it was drastically smaller than that of pristine UiO-68.

In addition, the photocurrent responses of **1**, **2**, and amorphous TiO_2 were studied (Figure 2). A three-electrode photoelectrochemical cell was built with the photoanode **1** or **2** as the working electrode, Ag/AgCl as the reference electrode, and platinum wire as the cathode for the visible-light-driven water splitting. An external bias of 0.7 V (vs NHE) was applied, and the photocurrents in a 0.1 M Na_2SO_4 aqueous solution (pH = 6.4) electrolyte were measured. Obviously, **2** showed a much higher photocurrent density than **1** upon light irradiation. Under the same conditions, the photocurrent of the free amorphous TiO_2 was also examined, and the results showed no difference whether it was irradiated or not. This clearly implied that the synergistic effect of **1** and TiO_2 in **2** significantly improved the separation efficiency of photo-generated electrons and holes.

Alcohol Oxidation Catalyzed by 2. Taking advantage of the photoactive TiO_2@MOF species, the photocatalytic oxidation activity of **2** was examined. To optimize the reaction conditions, benzyl alcohol oxidation in MeOH was chosen as the model reaction. As shown in Table 1, various catalytic oxidation conditions (Table 1, entries 1−10) were explored in an oxygen or air atmosphere using a polar solvent as the reaction medium to furnish the desired product. Table 1 (entry 1) demonstrated that the benzyl alcohol oxidation was a visible-light-triggered reaction, and basically no benzaldehyde was obtained in the absence of light irradiation.

In addition, only 11% yield of benzaldehyde was generated in the presence of **2** under natural sunlight irradiation in oxygen at ambient temperature (Table 1, entry 2). The best catalytic result (78% yield) was observed when the reaction was conducted in oxygen using 300 W xenon lamp ($\lambda > 400$ nm) as the visible-light source with aid of 1 mol % **2** (Table 1, entry 3). In air, the oxidation yield was down to 21% (Table 1, entry 4), indicating that pure oxygen is important to this benzyl alcohol oxidation. In addition, the different solvent systems were also examined (Table 1, entries 5−7), and 44−77% yields were obtained when the reaction was conducted in acetonitrile (CH_3CN), H_2O, and THF, respectively. The control experiment (Table 1, entry 8) showed that basically no conversion was observed (less than 1% yield) when **1** was used instead of **2** to perform the reaction. Furthermore, when free amorphous TiO_2 was employed, the desired oxidation product was generated in only 10% yield (ca. 90% starting alcohol was recovered) under the given conditions (Table 1, entry 9). On the other hand, the simple physical blend of **1** with amorphous TiO_2 also resulted in a very low oxidation yield at <12% (ca. 87% starting alcohol was recovered; Table 1, entry 10), which is well consistent with the photocurrent measurement given above.

On the basis of the optimized conditions, the scope and generality of photocatalytic oxidation by **2** were verified through different types of substituted benzyl alcohols (Table 2, entries 1−10). As shown in Table 2, all of the benzyl alcohols with electron-donating groups such as alkoxy (Table 2, entries 2−4; 90−>99% yields) and alkyl (Table 2, entries 5−7; 86−93% yields) groups employed under the optimized conditions furnished good-to-excellent yields within 24 h at room temperature. In contrast, the electron-withdrawing-group-attached substrates showed much lower activity for the oxidation (Table 2, entries 8−10; 35−45% yields). So, the electronic effect of the substituents appeared to be important for this **2**-catalyzed photocatalytic oxidation. As is known, the electron-donating substituents could lead to electron-rich benzylic alcohols, which would facilitate their oxidation,[53−55] consequently enhancing the catalytic efficiency of **2**.

MBH Reaction Catalyzed by 2. As is known, the MBH reaction can be catalyzed by the IL-bound quinuclidine in a homogeneous way.[56] So, we wondered if the L-pyrrolidine-2-ylimidazole-decorated **2** could also promote MBH reaction but in a heterogeneous manner, moreover, with high enantioselectivity.

For this, the reaction of methyl acrylate with benzaldehyde was chosen as the model reaction. Optimization of the reaction was first performed at different temperatures such as 25, 50, and 60 °C to furnish the desired MBH product under the given reaction conditions (Table 3, entries 1−3) in the same reaction time length (24 h). It seems that the higher temperature could be a benefit for increasing the MBH yields (25 °C, 44%; 50 °C, 79%; 60 °C, 87%), but it led to lower stereoselectivity (25 °C, 86% ee; 50 °C, 11% ee; 60 °C, <3% ee). To our delight, a facile reaction (Table 3, entry 4) occurred at room temperature (25 °C) at an extended reaction time (48 h) but with an excellent yield (96%) and a satisfied ee value (83%). In addition, when different solvents (cf. THF, H_2O, and CH_3CN) were employed in the presence of 2 mol % **2**, the desired product was obtained in low yields (10−66%) with ee values in the range of 65−83% (Table 3, entries 5−7). Furthermore, when the reaction was carried out in MeOH with a lower catalyst loading, 1.5 mol % instead of 2.0 mol %, the product was isolated in a slightly lower 93% yield, but with the obviously decreased ee value of 64% (Table 3, entry 8). On the other hand, the higher catalyst loading (2.5 mol %) did not affect the results significantly (Table 3, entry 9). Notably, the involved TiO_2 species did not disturb the MBH reaction between methyl acrylate and benzaldehyde under the given conditions, which was further supported by the control experiment in the presence of **1**. As shown in Table 3 (entry 10), when **1** was used instead of **2** at the same catalyst loading, the MBH product was obtained at the same yield (96%) and ee value (83%). Again, no effective conversion (<5% yield) and enantiomeric excess (<1% ee) were obtained without the aid of a catalyst (Table 3, entry 11).

We next explored the reaction scope under the optimized conditions, and the results are summarized in Table 4. The benzaldehydes with electron-donating substituents gave higher yields (Table 4, entries 1−6), while for those substrates containing electron-withdrawing substituents on the benzene ring (Table 4, entries 7−9), lower yields were obtained. For all substituted benzaldehydes, the 2-substituted substrates always gave relatively lower yields (Table 4, entries 1, 4, and 7), which clearly resulted from the ortho sterically hindered effect. For stereoselectivity, all of the substrates, however, exhibited good-to-excellent ee values (85−99%). So far, MOF-based MBH catalytic reactions remain quite rare, and a handful MOFs that can promote MBH reactions have appeared in the literature.[57−59] Among the reported MOF-based catalysts, only L_{Cu}PRO, together with an imidazole cocatalyst, was able to catalyze asymmetric MBH reactions but with very low ee values (5−8%).[59]

One-Pot MBH Reactions Catalyzed by 2. Considering the above results, we finally explored the possibility of **2**-catalyzed one-pot MBH reactions starting from benzyl alcohols and acrylic esters (Table 5, entries 1−11). In this context, 4-methoxybenzyl alcohol and methyl methacrylate were chosen as the starting substrates for this one-pot MBH reaction (Table 5, entry 4). When the reaction was carried out in an oxygen atmosphere with visible light (300 W xenon lamp) at room temperature for 72 h (monitored by TLC), 96% yield of the desired product was obtained. However, when the reaction was carried out in a sequential one-pot procedure instead, the corresponding yield increased to 99%. The slight difference might demonstrate that the **2**-catalyzed benzyl alcohol oxidation and the following MBH reaction in due succession could effectively avoid the possible side photoinduced polymerization of acrylic ester during the process.

The scope of the bifunctional catalytic system was further investigated by performing the oxidation−MBH reaction for other various substituted benzyl alcohols in a stepwise way. As shown in Table 5, the substituent effect on the tandem reaction was the same as those of the individual reaction steps. As shown, benzyl alcohols with electron-donating substituents have relatively higher yields (50−99%; Table 5, entries 1−7). However, low yields were obtained (12−27%; Table 5, entries 8−10) for those substrates containing electron-withdrawing substituents on the benzyl alcohols. Again, the steric hindrance effect still played an important role in the reaction efficiency. Compared to 2-substituted benzyl alcohols (yields 12−67%; Table 5, entries 2, 5, and 8), the 3- and 4-substituted ones displayed more activity and provided higher reaction yields, 16−99% (Table 5, entries, 3, 4, 6, 7, 9, and 10). Notably, all of the substrates exhibited good-to-excellent stereoselectivities (81−99%), suggesting that the chiral **1** framework showed an excellent asymmetric templating effect to arrange the reaction substrates and induce their contact in the specific spatial orientations. It is noteworthy that large-sized substrates such as 9-anthracenemethanol did not afford the expected product because no corresponding 9-anthraldehyde was detected (Table 5, entry 11). This suggested that internal surface catalysis should be the dominant process; moreover, the involved amorphous TiO_2 species was indeed located inside the MOF matrix.

To verify the heterogeneous catalysis nature and stability of **2**, a hot leaching test was carried out on the model reaction of 4-methoxybenzyl alcohol with methyl acrylate (Table 5, entry 4). As shown in Figure 3a, no further reaction occurred without **2** after ignition of the reaction at 48 h, indicating that no leaching of the catalytically active sites occurred and that **2** featured a typical heterogeneous catalyst nature. In addition, we also examined the recyclability of **2**. After each catalytic run, the solid catalyst of **2** was collected by centrifugation, washed with MeOH, dried at 80 °C, and reused in the next run under the same conditions. Within five catalytic runs, 96−99% yields were obtained with 99% stereoselectivity (Figure 3b).

The PXRD patterns and SEM image of **2** after five catalytic runs showed that the structural integrity and morphology of **2** were well-preserved (Figure 3c,d), and the dispersion of the loaded TiO_2 species was still uniform in **2** based on the EDS elemental mapping (Figure 3d). The TiO_2 loss is only 8.2% after five catalytic runs (determined by ICP atomic emission spectrometry; see the Supporting Information). Thus, **1** could be considered to be an ideal host platform to load TiO_2, and **2** is a satisfied bifunctional chiral heterogeneous catalyst for the synthesis of asymmetric MBH additive products from alcohols and methyl acrylate via a one-pot sequential reaction. To our knowledge, this is the first example for one-pot tandem MBH reactions promoted by the chiral MOF-based composite catalyst.

■ CONCLUSIONS

In summary, we have demonstrated a facile synthetic method for the preparation of a MOF-based multifunctional heterogeneous catalytic material, in which the chiral organic catalytic and photoactive TiO_2 species were successfully and rationally combined via a MOF platform. The obtained chiral **2** can be a highly active bifunctional asymmetric heterogeneous catalyst to promote both photodriven and thermal-driven reaction in a stepwise way under mild conditions. In this way, the asymmetric one-pot MBH reaction starting from benzyl alcohols was finally realized. We expect this approach to be viable for the construction of many more new multifunctional MOF-based catalytic systems for tandem chemical transformation.

■ ASSOCIATED CONTENT

Ⓢ Supporting Information

The Supporting Information is available free of charge on the ACS Publications website at DOI: 10.1021/acs.inorgchem.8b02132.

> Synthesis and characterization of **H_2L-CIL**, additional characterization of **2**, and MBH product characterization (PDF)

■ AUTHOR INFORMATION

Corresponding Authors

*E-mail: wangjiancheng1003@163.com.
*E-mail: yubindong@sdnu.edu.cn.

ORCID

Yu-Bin Dong: 0000-0002-9698-8863

Author Contributions

[†]These authors contributed equally.

Notes

The authors declare no competing financial interest.

■ ACKNOWLEDGMENTS

We are grateful for financial support from the NSFC (Grants 21671122, 21475078, and 21802090), Shandong Provincial Natural Science Foundation (Grant ZR2018BB006), a Project of the Shandong Province Higher Educational Science and Technology Program (J18KA066), and the Taishan Scholar's Construction Project.

■ REFERENCES

(1) Corma, A.; García, H.; Llabrés i Xamena, F. X. Engineering Metal Organic Frameworks for Heterogeneous Catalysis. *Chem. Rev.* **2010**, *110*, 4606−4655.

(2) Zhu, L.; Liu, X.-Q.; Jiang, H.-L.; Sun, L.-B. Metal−Organic Frameworks for Heterogeneous Basic Catalysis. *Chem. Rev.* **2017**, *117*, 8129−8176.

(3) Yoon, M.; Srirambalaji, R.; Kim, K. Homochiral Metal−Organic Frameworks for Asymmetric Heterogeneous Catalysis. *Chem. Rev.* **2012**, *112*, 1196−1231.

(4) Falcaro, P.; Ricco, R.; Yazdi, A.; Imaz, I.; Furukawa, S.; Maspoch, D.; Ameloot, R.; Evans, J. D.; Doonan, C. J. Application of metal and metal oxide nanoparticles@MOFs. *Coord. Chem. Rev.* **2016**, *307*, 237−254.

(5) Moon, H. R.; Lim, D.-W.; Suh, M. P. Fabrication of Metal Nanoparticles in Metal-Organic Frameworks. *Chem. Soc. Rev.* **2013**, *42*, 1807−1824.

(6) Zhao, M.; Yuan, K.; Wang, Y.; Li, G.; Guo, J.; Gu, L.; Hu, W.; Zhao, H.; Tang, Z. Metal-Organic Frameworks as Selectivity Regulators for Hydrogenation Reactions. *Nature* **2016**, *539*, 76−80.

(7) Müller, M.; Hermes, S.; Kähler, K.; van den Berg, M. W. E.; Muhler, M.; Fischer, R. A. Loading of MOF-5 with Cu and ZnO Nanoparticles by Gas-Phase Infiltration with Organometallic Precursors: Properties of Cu/ZnO@MOF-5 as Catalyst for Methanol Synthesis. *Chem. Mater.* **2008**, *20*, 4576−4587.

(8) Limvorapitux, R.; Chou, L.-Y.; Young, A. P.; Tsung, C.-K.; Nguyen, S. T. Coupling Molecular and Nanoparticle Catalysts on Single Metal−Organic Framework Microcrystals for the Tandem Reaction of H_2O_2 Generation and Selective Alkene Oxidation. *ACS Catal.* **2017**, *7*, 6691−6698.

(9) Chen, Y.-Z.; Wang, Z. U.; Wang, H.; Lu, J.; Yu, S.-H.; Jiang, H.-L. Singlet Oxygen-Engaged Selective Photo-Oxidation over Pt Nanocrystals/Porphyrinic MOF: The Roles of Photothermal Effect and Pt Electronic State. *J. Am. Chem. Soc.* **2017**, *139*, 2035−2044.

(10) Zhu, Q.-L.; Li, J.; Xu, Q. Immobilizing Metal Nanoparticles to Metal−Organic Frameworks with Size and Location Control for Optimizing Catalytic Performance. *J. Am. Chem. Soc.* **2013**, *135*, 10210−10213.

(11) Zeng, T.; Zhang, X.; Wang, S.; Niu, H.; Cai, Y. Spatial Confinement of a Co_3O_4 Catalyst in Hollow Metal−Organic Frameworks as a Nanoreactor for Improved Degradation of Organic Pollutants. *Environ. Sci. Technol.* **2015**, *49*, 2350−2357.

(12) An, B.; Zhang, J.; Cheng, K.; Ji, P.; Wang, C.; Lin, W. Confinement of Ultrasmall Cu/ZnOx Nanoparticles in Metal−Organic Frameworks for Selective Methanol Synthesis from Catalytic Hydrogenation of CO_2. *J. Am. Chem. Soc.* **2017**, *139*, 3834−3840.

(13) Li, Y.-A.; Yang, S.; Liu, Q.-K.; Chen, G.-J.; Ma, J.-P.; Dong, Y.-B. Pd(0)@UiO-68-AP: Chelating-Directed Bifunctional Heterogeneous Catalyst for Stepwise Organic Transformations. *Chem. Commun.* **2016**, *52*, 6517−6520.

(14) Chen, G.-J.; Ma, H.-C.; Xin, W.-L.; Li, X.-B.; Jin, F.-Z.; Wang, J.-S.; Liu, M.-Y.; Dong, Y.-B. Dual Heterogeneous Catalyst Pd-Au@Mn(II)-MOF for One-Pot Tandem Synthesis of Imines from Alcohols and Amines. *Inorg. Chem.* **2017**, *56*, 654−660.

(15) Wang, H.-L.; Yeh, H.; Chen, Y.-C.; Lai, Y.-C.; Lin, C.-Y.; Lu, K.-Y.; Ho, R.-M.; Li, B.-H.; Lin, C.-H.; Tsai, D.-H. Thermal Stability of Metal−Organic Frameworks and Encapsulation of CuO Nanocrystals for Highly Active Catalysis. *ACS Appl. Mater. Interfaces* **2018**, *10*, 9332−9341.

(16) Noh, H.; Kung, C.-W.; Islamoglu, T.; Peters, A. W.; Liao, Y.; Li, P.; Garibay, S. J.; Zhang, X.; DeStefano, M. R.; Hupp, J. T.; Farha, O. K. Room Temperature Synthesis of an 8-Connected Zr-Based Metal−Organic Framework for Top-Down Nanoparticle Encapsulation. *Chem. Mater.* **2018**, *30*, 2193−2197.

(17) Shultz, A. M.; Sarjeant, A. A.; Farha, O. K.; Hupp, J. T.; Nguyen, S. T. Post-Synthesis Modification of a Metal−Organic Framework to Form Metallosalen-Containing MOF Materials. *J. Am. Chem. Soc.* **2011**, *133*, 13252−13255.

(18) Madrahimov, S. T.; Gallagher, J. R.; Zhang, G.; Meinhart, Z.; Garibay, S. J.; Delferro, M.; Miller, J. T.; Farha, O. K.; Hupp, J. T.; Nguyen, S. T. Gas-Phase Dimerization of Ethylene under Mild Conditions Catalyzed by MOF Materials Containing (bpy)NiII Complexes. *ACS Catal.* **2015**, *5*, 6713−6718.

(19) Hu, Y.-H.; Wang, J.-C.; Yang, S.; Li, Y.-A.; Dong, Y.-B. CuI@UiO-67-IM: A MOF-Based Bifunctional Composite Triphase Transfer Catalyst for Sequential One-Pot Azide−Alkyne Cycloaddition in Water. *Inorg. Chem.* **2017**, *56*, 8341−8347.

(20) Wang, J.-C.; Hu, Y.-H.; Chen, G.-J.; Dong, Y.-B. Cu(II)/Cu(0)@UiO-66-NH_2: base metal@MOFs as heterogeneous catalysts for

olefin oxidation and reduction. *Chem. Commun.* **2016**, *52*, 13116−13119.

(21) Wei, Y.-L.; Li, Y.; Chen, Y.-Q.; Dong, Y.; Yao, J.-J.; Han, X.-Y.; Dong, Y.-B. Pd(II)-NHDC-Functionalized UiO-67 Type MOF for Catalyzing Heck Cross-Coupling and Intermolecular Benzyne−Benzyne−Alkene Insertion Reactions. *Inorg. Chem.* **2018**, *57*, 4379−4386.

(22) Zhu, N.-X.; Zhao, C.-W.; Wang, J.-C.; Li, Y.-A.; Dong, Y.-B. Micro-Cu_4I_4-MOF: reversible iodine adsorption and catalytic properties for tandem reaction of Friedel−Crafts alkylation of indoles with acetals. *Chem. Commun.* **2016**, *52*, 12702−12705.

(23) Zhang, X.-M.; Zhao, C.-W.; Ma, J.-P.; Yu, Y.; Liu, Q.-K.; Dong, Y.-B. *Chem. Commun.* **2015**, *51*, 839−842.

(24) Goossens, K.; Lava, K.; Bielawski, C. W.; Binnemans, K. Ionic Liquid Crystals: Versatile Materials. *Chem. Rev.* **2016**, *116*, 4643−4807.

(25) Amarasekara, A. S. Acidic Ionic Liquids. *Chem. Rev.* **2016**, *116*, 6133−6183.

(26) Wilcox, R. J.; Losey, B. P.; Folmer, J. C. W.; Martin, J. D.; Zeller, M.; Sommer, R. Crystalline and Liquid Structure of Zinc Chlorid Trihydrate: A Unique Ionic Liquid. *Inorg. Chem.* **2015**, *54*, 1109−1119.

(27) Luo, S.; Mi, X.; Zhang, L.; Liu, S.; Xu, H.; Cheng, J.-P. Functionalized ionic liquids catalyzed direct aldol reactions. *Tetrahedron* **2007**, *63*, 1923−1930.

(28) Wang, J.-C.; Ma, J.-P.; Liu, Q.-K.; Hu, Y.-H.; Dong, Y.-B. Cd(II)-MOF-IM: Post-Synthesis Functionalization of Cd(II)-MOF for Triphase Transfer Catalyst. *Chem. Commun.* **2016**, *52*, 6989−6992.

(29) Ding, L.-G.; Yao, B.-J.; Jiang, W.-L.; Li, J.-T.; Fu, Q.-J.; Li, Y.-A.; Liu, Z.-H.; Ma, J.-P.; Dong, Y.-B. Bifunctional Imidazolium-Based Ionic Liquid Decorated UiO-67 Type MOF for Selective CO_2 Adsorption and Catalytic Property for CO_2 Cycloaddition with Epoxides. *Inorg. Chem.* **2017**, *56*, 2337−2344.

(30) Yao, B.-J.; Ding, L.-G.; Li, F.; Li, J.-T.; Fu, Q.-J.; Ban, Y.; Guo, A.; Dong, Y.-B. Chemically Cross-Linked MOF Membrane Generated from Imidazolium-Based Ionic Liquid-Decorated UiO-66 Type NMOF and Its Application toward CO_2 Separation and Conversion. *ACS Appl. Mater. Interfaces* **2017**, *9*, 38919−38930.

(31) Liang, J.; Chen, R.-P.; Wang, X.-Y.; Liu, T.-T.; Wang, X.-S.; Huang, Y.-B.; Cao, R. Postsynthetic ionization of an imidazole containing metal−organic framework for the cycloaddition of carbon dioxide and epoxides. *Chem. Sci.* **2017**, *8*, 1570−1575.

(32) O'Regan, B.; Gratzel, M. A Low-Cost, High-Efficiency Solar Cell Based on Dye-Sensitized Colloidal TiO_2 Films. *Nature* **1991**, *353*, 737−740.

(33) Wang, P.; Zakeeruddin, S. M.; Humphry-Baker, R.; Moser, J. E.; Gratzel, M. Molecular-Scale Interface Engineering of TiO_2 Nanocrystals: Improve the Efficiency and Stability of Dye-Sensitized Solar Cells. *Adv. Mater.* **2003**, *15*, 2101−2104.

(34) Nakade, S.; Matsuda, M.; Kambe, S.; Saito, Y.; Kitamura, T.; Sakata, T.; Wada, Y.; Mori, H.; Yanagida, S. Dependence of TiO_2 Nanoparticle Preparation Methods and Annealing Temperature on the Efficiency of Dye-Sensitized Solar Cells. *J. Phys. Chem. B* **2002**, *106*, 10004−10010.

(35) Zhao, C.-W.; Li, Y.-A.; Wang, X.-R.; Chen, G.-J.; Liu, Q.-K.; Ma, J.-P.; Dong, Y.-B. Fabrication of Cd(II)-MOF-based ternary photocatalytic composite materials for H_2 production via a gel-to-crystal approach. *Chem. Commun.* **2015**, *51*, 15906−15909.

(36) Hoffmann, M. R.; Martin, S. T.; Choi, W.; Bahnemann, D. W. Environmental Applications of Semiconductor Photocatalysis. *Chem. Rev.* **1995**, *95*, 69−96.

(37) Gao, L.; Zhang, Q. H. Effects of amorphous contents and particle size on the photocatalytic properties of TiO_2 nanoparticles. *Scr. Mater.* **2001**, *44*, 1195−1198.

(38) Chae, S. Y.; Park, M. K.; Lee, S. K.; Kim, T. Y.; Kim, S. K.; Lee, W. I. Preparation of Size-Controlled TiO_2 Nanoparticles and Derivation of Optically Transparent Photocatalytic Films. *Chem. Mater.* **2003**, *15*, 3326−3331.

(39) Naoi, K.; Ohko, Y.; Tatsuma, T. TiO_2 Films Loaded with Silver Nanoparticles: Control of Multicolor Photochromic Behavior. *J. Am. Chem. Soc.* **2004**, *126*, 3664−3668.

(40) Ohko, Y.; Tatsuma, T.; Fujii, T.; Naoi, K.; Niwa, C.; Kubota, Y.; Fujishima, A. Multicolour photochromism of TiO_2 films loaded with silver nanoparticles. *Nat. Mater.* **2003**, *2*, 29−31.

(41) Zhu, Y.; Shi, J.; Zhang, Z.; Zhang, C.; Zhang, X. Development of a Gas Sensor Utilizing Chemiluminescence on Nanosized Titanium Dioxide. *Anal. Chem.* **2002**, *74*, 120−124.

(42) Wu, N.; Wang, S.; Rusakova, I. A. Inhibition of crystallite growth in the sol−gel synthesis of nanocrystalline metal oxides. *Science* **1999**, *285*, 1375−1377.

(43) Kutzscher, C.; Nickerl, G.; Senkovska, I.; Bon, V.; Kaskel, S. Proline Functionalized UiO-67 and UiO-68 Type Metal-Organic Frameworks Showing Reversed Diastereoselectivity in Aldol Addition Reactions. *Chem. Mater.* **2016**, *28*, 2573−2580.

(44) Mo, K.; Yang, Y.; Cui, Y. A Homochiral Metal−Organic Framework as an Effective Asymmetric Catalyst for Cyanohydrin Synthesis. *J. Am. Chem. Soc.* **2014**, *136*, 1746−1749.

(45) Wu, C.-D.; Hu, A.; Zhang, L.; Lin, W. A Homochiral Porous Metal-Organic Framework for Highly Enantioselective Heterogeneous Asymmetric Catalysis. *J. Am. Chem. Soc.* **2005**, *127*, 8940−8941.

(46) Wanderley, M. M.; Wang, C.; Wu, C.-D.; Lin, W. A Chiral Porous Metal−Organic Framework for Highly Sensitive and Enantioselective Fluorescence Sensing of Amino Alcohols. *J. Am. Chem. Soc.* **2012**, *134*, 9050−9053.

(47) Ichijo, T.; Sato, S.; Fujita, M. Size-, Mass-, and Density-Controlled Preparation of TiO2 Nanoparticles in a Spherical Coordination Template. *J. Am. Chem. Soc.* **2013**, *135*, 6786−6789.

(48) Yang, Q. Y.; Guillerm, V.; Ragon, F.; Wiersum, A. D.; Llewellyn, P. L.; Zhong, C.-L.; Devic, T.; Serre, C.; Maurin, G. CH_4 storage and CO_2 capture in highly porous zirconium oxide based metal−organic frameworks. *Chem. Commun.* **2012**, *48*, 9831−9833.

(49) Cavka, J. H.; Jakobsen, S.; Olsbye, U.; Guillou, N.; Lamberti, C.; Bordiga, S.; Lillerud, K. P. A New Zirconium Inorganic Building Brick Forming Metal Organic Frameworks with Exceptional Stability. *J. Am. Chem. Soc.* **2008**, *130*, 13850−13851.

(50) Abedi, S.; Karimi, B.; Kazemi, F.; Bostina, M.; Vali, H. Amorphous TiO_2 coated into periodic mesoporous organosilicate channels as a new binary photocatalyst for regeneration of carbonyl compounds from oximes under sunlight irradiation. *Org. Biomol. Chem.* **2013**, *11*, 416−419.

(51) Abedi, S.; Morsali, A. Ordered Mesoporous Metal−Organic Frameworks Incorporated with Amorphous TiO_2 As Photocatalyst for Selective Aerobic Oxidation in Sunlight Irradiation. *ACS Catal.* **2014**, *4*, 1398−1403.

(52) Yan, W.; Mahurin, M.; Overbury, S. H.; Dai, S. Nonhydrolytic Layer-by-Layer Surface Sol−Gel Modification of Powdered Mesoporous Silica Materials with TiO_2. *Chem. Mater.* **2005**, *17*, 1923−1925.

(53) Fujita, K.; Yoshida, T.; Imori, Y.; Yamaguchi, R. Dehydrogenative Oxidation of Primary and Secondary Alcohols Catalyzed by a Cp*Ir Complex Having a Functional C, N-Chelate Ligand. *Org. Lett.* **2011**, *13*, 2278−2281.

(54) Mazloomi, Z.; Pretorius, R.; Pàmies, O.; Albrecht, M.; Diéguez, M. Triazolylidene Iridium Complexes for Highly Efficient and Versatile Transfer Hydrogenation of C=O, C=N, and C=C Bonds and for Acceptorless Alcohol Oxidation. *Inorg. Chem.* **2017**, *56*, 11282−11298.

(55) Sinha, S.; Das, S.; Sikari, R.; Parua, S.; Brandao, P.; Demeshko, S.; Meyer, F.; Paul, N. D. Redox Noninnocent Azo-Aromatic Pincers and Their Iron Complexes. Isolation, Characterization, and Catalytic Alcohol Oxidation. *Inorg. Chem.* **2017**, *56*, 14084−14100.

(56) Mi, X.-L.; Luo, S.-Z.; Cheng, J.-P. Ionic Liquid-Immobilized Quinuclidine-Catalyzed Morita-Baylis-Hillman Reactions. *J. Org. Chem.* **2005**, *70*, 2338−2341.

(57) Sharma, v.; De, D.; Pal, S.; Saha, P.; Bharadwaj, P. K. A 2D Coordination Network That Detects Nitro Explosives in Water,

DOI: 10.1021/acs.inorgchem.8b02132
Inorg. Chem. XXXX, XXX, XXX−XXX

Catalyzes Baylis–Hillman Reactions, and Undergoes Unusual 2D→3D Single-Crystal to Single-Crystal Transformation. *Inorg. Chem.* **2017**, *56*, 8847–8855.

(58) Bauer, G.; Ongari, D.; Xu, X.-Y.; Tiana, D.; Smit, B.; Ranocchiari, M. Metal–Organic Frameworks Invert Molecular Reactivity: Lewis Acidic Phosphonium Zwitterions Catalyze the Aldol-Tishchenko Reaction. *J. Am. Chem. Soc.* **2017**, *139*, 18166–18169.

(59) De, D.; Pal, T. K.; Bharadwaj, P. K. A Porous Cu (II)-MOF with Proline Embellished Cavity: Cooperative Catalysis for the Baylis - Hillman Reaction. *Inorg. Chem.* **2016**, *55*, 6842–6844.

DOI: 10.1021/acs.inorgchem.8b02132
Inorg. Chem. XXXX, XXX, XXX–XXX